Dielectric Properties of Solid Molecular Hydrogen at High Pressure

Alberto García and Marvin L. Cohen
Department of Physics, University of California, Berkeley, Berkeley, California 94720
and Materials Sciences Division, Lawrence Berkeley Laboratory, Berkeley, California 94720

Jon H. Eggert, Fred Moshary, William J. Evans,
Kenneth A. Goettel, and Isaac F. Silvera
Lyman Laboratory of Physics, Harvard University, Cambridge, Massachussetts 02138
(Received 21 August 1991; revised manuscript received 11 October 1991)

We present experimental data on the dielectric behavior of solid molecular hydrogen to pressures up to 220 GPa. To complement these measurements, a calculation of the interband dielectric response was done for two prototype structures of hcp molecular solid hydrogen. It is shown that this theoretical approach allows a more complete analysis of the experimental data on compressed solid molecular hydrogen than previously possible.

I. INTRODUCTION

The prediction of the metallization pressure of hydrogen has been a theoretical challenge since the proposal[1] in 1935 that at sufficiently high pressure hydrogen would transform from an insulating molecular solid into a metallic atomic solid. It is now hypothesized that hydrogen can first metallize in the molecular state by a band overlap mechanism. Evidence for this was first provided by calculations based on an assumed $Pa3$ crystal structure.[2–4] However, according to x-ray and neutron diffraction experiments,[5–7] the room-temperature structure of solid hydrogen and deuterium to moderately high pressures is hexagonal close packed (hcp). Subsequent total-energy calculations[8] demonstrated that a prototype hcp structure is more stable than the $Pa3$ arrangement in the pressure range of interest. In this arrangement [which we will refer to as mhcp(O) in the following; (O) signifies oriented] the hydrogen molecules are centered on the sites of the hcp structure, with their axes aligned parallel to the hexagonal axis. For this structure, the closing of an indirect band gap upon compression was also shown to occur, but at significantly lower pressures than those reported for the $Pa3$ structure.[9]

On the experimental side, some evidence for a metallic molecular phase of solid hydrogen has been reported. In 1988 a phase transition was observed[10] at about 150 GPa, which was thought to be an extension of the well-known low-pressure transition to orientational ordering of the molecules due to electric quadrupole-quadrupole interactions. Later it was found[11] that this transition only existed above 149 GPa and it was attributed to a new phase (hydrogen-A) unrelated to the low-pressure phase. Subsequently, claims of metallization of hydrogen at 148 GPa have been made based on the observation of a rising edge in the ir reflectivity and absorption, which was studied to pressures up to 177 GPa and assigned to a free electron Drude edge.[12,13] However, other studies of optical reflectivity and absorption up to 230 GPa have failed to confirm these observations and interpretation of metallic behavior.[14] It has been speculated that the reported rising edge might be due to an impurity in the sample such as ruby reacting with hydrogen.[15]

For a comparison of the computed metallization pressure and the experimental value to be meaningful, proper consideration should be given to the limitations of the theoretical approaches. In particular, the use of the local-density approximation (LDA) for exchange and correlation is inadequate, since the LDA is known to underestimate the band gaps of semiconductors and insulators.[16] One attempt to correct this undesirable feature is the use of a semiempirical model for the exchange and correlation potential.[17] This scheme predicts a metallization pressure of 180(20) GPa for the prototype mhcp(O) structure, and a much higher value (approximately 400 GPa), for an idealized model with spherical charge distributions at the molecular sites [referred to as mhcp(S)].[17] All of the significant results obtained with the use of this semiempirical approach have been qualitatively confirmed by a more sophisticated quasiparticle calculation.[18]

If only comparisons between predicted and experimentally determined metallization pressures are done, a great deal of information is neglected, since optical experiments typically probe the overall dielectric behavior of the solid hydrogen samples. Hence, a more complete understanding is possible if the dielectric response is modeled theoretically. Here we present experimental data on the dielectric response of solid hydrogen to 220 GPa in the visible part of the spectrum. In order to interpret these data, we have calculated the interband contribution to the dielectric properties of two prototype structures [the mhcp(O) and mhcp(S) arrangements] as a function of density. These structures are meant to be representative, since the structure of solid hydrogen in this pressure

range has not been determined.

The experimental work described below has pushed forward the range of pressures for which the dielectric properties of hydrogen have been studied. Earlier Shimizu *et al.*[19] measured the index of refraction to about 20 GPa using Brillouin scattering. van Straaten, Wijngaarden, and Silvera[20] introduced the Fabry-Pérot technique in the diamond anvil cell to measure the index to 37 GPa. Subsequently van Straaten and Silvera[21,22] measured the dispersion of hydrogen in the visible to 28 GPa. Eggert, Goettel, and Silvera[23] extended this work to 73 GPa. Using the same technique, Hemley, Hanfland, and Mao[24] determined single oscillator frequencies into the megabar pressure range, which we have reanalyzed to obtain the dispersion.

II. EXPERIMENT

Hydrogen was cryogenically loaded into a diamond anvil cell (DAC) and optical studies were carried out up to 220 GPa at 77 K. Pressures were determined from the quasi-hydrostatic ruby pressure scale,[25] using fluorescence spectra from small ruby grains embedded in the edge of the hydrogen sample.

In a DAC the sample lies between two parallel faces of the diamond culets; the cavity formed by the two diamond-hydrogen interfaces forms a Fabry-Pérot (FP) resonator. We measured the FP fringes in reflection in the visible region of the optical spectra, for pressures up to 220 GPa. An example of the experimental data for the fringes can be seen in Ref. 14. The details of the method can be found elsewhere.[21–23] In principle, this measurement technique can yield both the index of refraction and its dispersion as a function of frequency and pressure,[21,22] however, in this work, because of geometrical constraints, we only determined the product $n_0 d$ of the index of refraction and the sample thickness and the ratio

$$C = (1/n_0)(dn/d\nu)_{\nu_0} \tag{1}$$

of the index and its dispersion. (The subscript 0 refers to magnitudes taken at the frequency $\nu_0 = 18\,000\ \mathrm{cm}^{-1}$.)

The magnitude C in Eq. (1) can be determined relatively accurately if the order of the fringes is known.[21,22] In our case the mean fringe order was about 28 and we could not unambiguously identify each fringe by its order. Instead of fitting to the Fabry-Pérot intensity equation, we used a sinusoid, which is a good approximation to the FP equation for low reflectivity, as is the case here:

$$I(\nu) = A\sin\{4\pi B[1 + (\nu - \nu_0)C]\nu + D\}. \tag{2}$$

Here A is the amplitude, $B = n_0 d$, and D is the phase. Before fitting, the data were Fourier filtered to remove the zero- and low-frequency components. The parameters were determined with a least-squares nonlinear fitting routine. This was done for all pressures studied, except in the region of 120 to 160 GPa, where the fringe contrast was very low because of index matching between the hydrogen and diamond.

III. THEORY

The various optical response constants can be calculated from the complex dielectric function, which in turn is obtained from the band structure. As in previous work,[17] the shortcomings of the LDA can be addressed through the use of a semiempirical model for the exchange and correlation potential. Here we choose the Slater $X\alpha$ scheme[26] and vary the strength parameter α to reproduce the main features of the experimentally determined[27] absorption at atmospheric pressure. The spectrum has an interband onset at approximately 15 eV and a broad shoulder at approximately 17 eV. We note that the value chosen in Ref. 17, namely, $\alpha = 1.56$, gives the same value for the direct gap in mhcp(O) as a first-principles quasiparticle calculation.[18] For mhcp(S) α is set at 1.44 to reproduce the corresponding zero-pressure quasiparticle gap.

We fixed the molecular bond length at the experimental value of approximately 1.4 a.u.[28] The c/a ratios were based on x-ray data,[5] with a high-density limit of 1.58. We use the Natarajan-Vanderbilt diagonalization scheme[29] to obtain the energy levels and wave functions from the secular equation, with a plane-wave basis and a 36 Ry cutoff.

Using first-order perturbation theory,[30] the imaginary component of the dielectric function is given by

$$\epsilon_2(\omega) = \frac{e^2}{\pi m^2 \omega^2} \sum_{v,c} \int_{BZ} d\mathbf{k} |\mathbf{e}\cdot\mathbf{M}_{cv}(\mathbf{k})|^2 \delta(E_c(\mathbf{k}) - E_v(\mathbf{k}) - \hbar\omega), \tag{3}$$

where

$$\mathbf{e}\cdot\mathbf{M}_{cv}(\mathbf{k}) = \langle \psi_{c\mathbf{k}} | \mathbf{e}\cdot\mathbf{p} | \psi_{v\mathbf{k}} \rangle \tag{4}$$

is the dipole matrix element. The subscripts v, c refer to valence and conduction bands, respectively, and $E_{v,c}(\mathbf{k})$ is the band energy. The integration is over wavevectors $\mathbf{k}$ in the Brillouin zone (BZ). Formally, the dielectric function is a second-rank tensor. For our prototype structures, if we take the z axis to coincide with the hexagonal axis, only two components need to be specified, namely, the zz and the $xx(= yy)$ components. These components are obtained by setting the unit vector $\mathbf{e}$ in Eq. (3) to $\hat{\mathbf{z}}$ and $\hat{\mathbf{x}}$, respectively. Note that both mhcp(O) and mhcp(S) share the same space group.

We use the tetrahedron method (enhanced to account for the $\mathbf{k}$-dependent matrix elements[31]) to compute the relevant BZ integration. The real part of the dielectric function is obtained by an application of the Kramers-Kronig relation

$$\epsilon_1(\omega) = 1 + \frac{1}{\pi} P \int_{-\infty}^{+\infty} \frac{\epsilon_2(\xi)}{\xi - \omega} d\xi. \quad (5)$$

The imaginary part of the dielectric function must satisfy the sum rule

$$\int_0^{\infty} \omega \epsilon_2(\omega) d\omega = \frac{\pi}{2} \omega_p^2, \quad (6)$$

where ω_p is the plasma frequency associated with the valence electrons. Since the number of bands taken into account in the sum in Eq. (3) is necessarily finite (20 in this work), the sum rule can only be approximately satisfied (to better than 80% in this case). It should be noted that in the calculation of the dielectric properties of interest $\epsilon_2(\omega)$ always appears integrated with negative powers of ω. This circumstance makes it possible to safely neglect the contribution of higher bands. This is not the case for the integral in Eq. (6), where $\epsilon_2(\omega)$ is weighted by ω, since this weighting magnifies the contribution of higher bands. Once both components of the dielectric function have been determined, the frequency-dependent complex index of refraction is given by the square root of the dielectric function.

As it is evident from the above, this calculation addresses only the contribution of interband transitions to the dielectric behavior. We have not considered the effects of the free carriers arising from the closing of the indirect band gap with increasing pressure [at approximately 180 GPa in mhcp(O) (Ref. 17)]. Also, the experimental absorption spectrum of solid molecular hydrogen[27] shows important excitonic effects. It is likely that a fraction of the total oscillator strength is associated with exciton absorption over the whole pressure range considered.

IV. RESULTS

We show in Figs. 1 and 2 the computed $\epsilon(\omega)$ for mhcp(O) at r_s=2.00 a.u.,[32] which corresponds to approximately 13 GPa,[33] and at r_s=1.60 a.u. (approximately 93 Gpa). A sizable anisotropy is evident from the comparison of ϵ_{zz} and ϵ_{xx}. This is expected on the basis of the orientation of the molecules: Similar plots of $\epsilon(\omega)$ for mhcp(S) (Figs. 3 and 4) show a greatly reduced anisotropy. A direct comparison with experiment can be carried out for pressures below 40 GPa (Refs. 19 and 34) for the index of refraction. The results are presented on Fig. 5. We note that there is fair agreement between the experimental results and the computed n_{zz} for mhcp(O). In contrast, n_{xx} deviates markedly, and so does the computed index for mhcp(S). No information is available about whether the samples used in Refs. 19 and 34 were single-crystal or polycrystalline.

Previous data on the dispersion of the index of refraction[34,23,24] can be brought into the form used here, namely, as the ratio $C = (1/n)dn/d\nu$, for the purpose of comparison.[35] Figure 6 shows the computed values for the magnitude C defined above as a function of den-

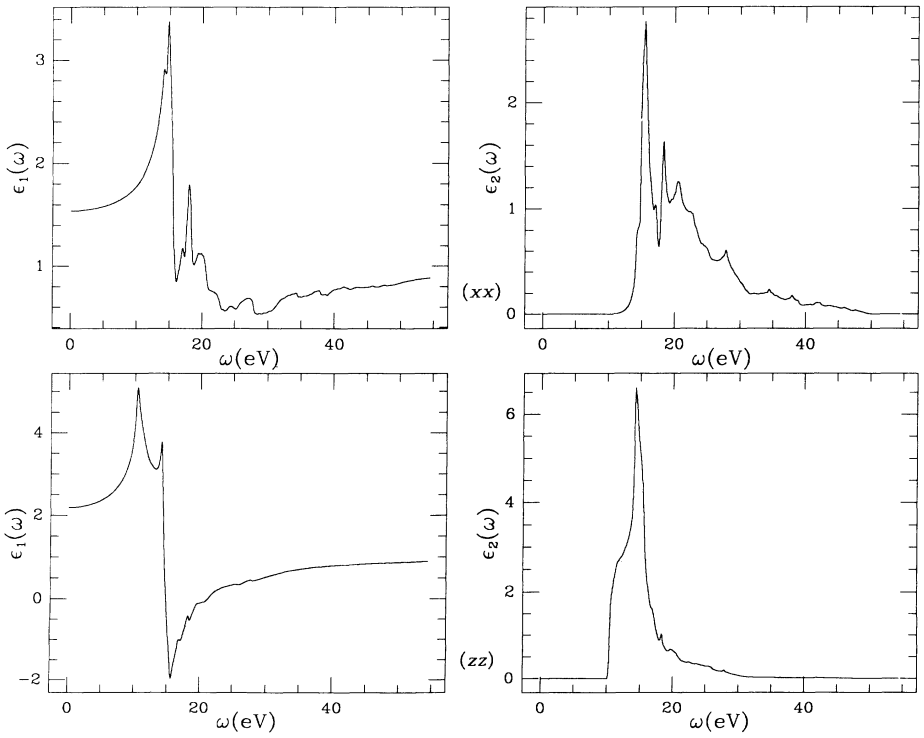

FIG. 1. Computed dielectric function for mhcp(O) at r_s=2.00 a.u. (corresponding to approximately 13 GPa). The top panels display the real (left) and imaginary (right) parts of $\epsilon_{xx}(\omega)$. The bottom panels present the same information for $\epsilon_{zz}(\omega)$.

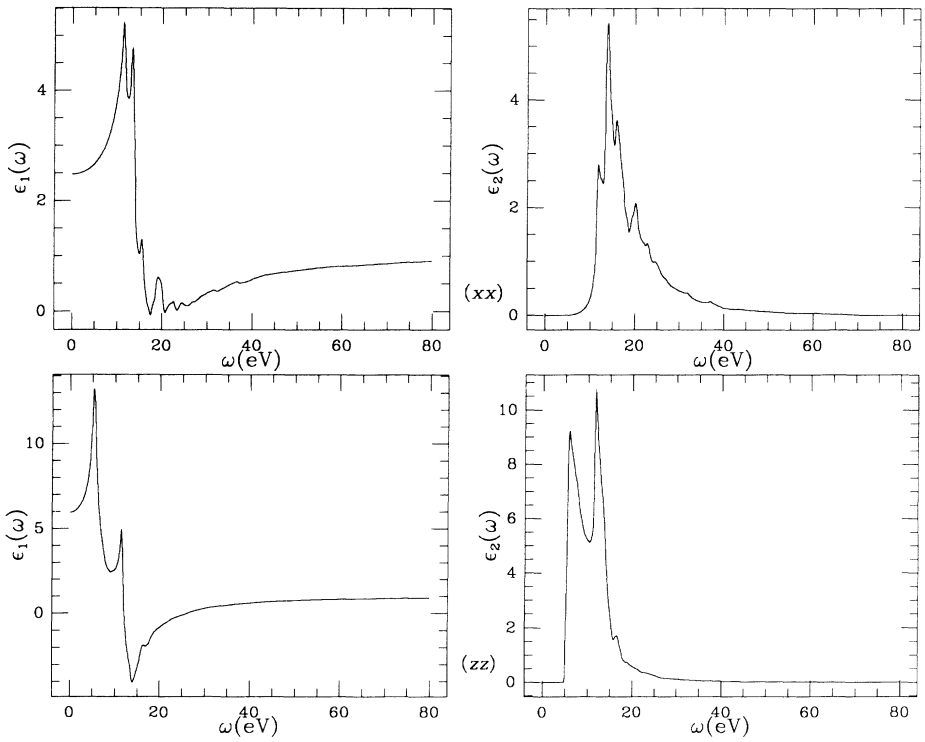

FIG. 2. Computed dielectric function for mhcp(O) at r_s=1.60 a.u. (corresponding to approximately 93 GPa). The top panels display the real (left) and imaginary (right) parts of $\epsilon_{xx}(\omega)$. The bottom panels present the same information for $\epsilon_{zz}(\omega)$.

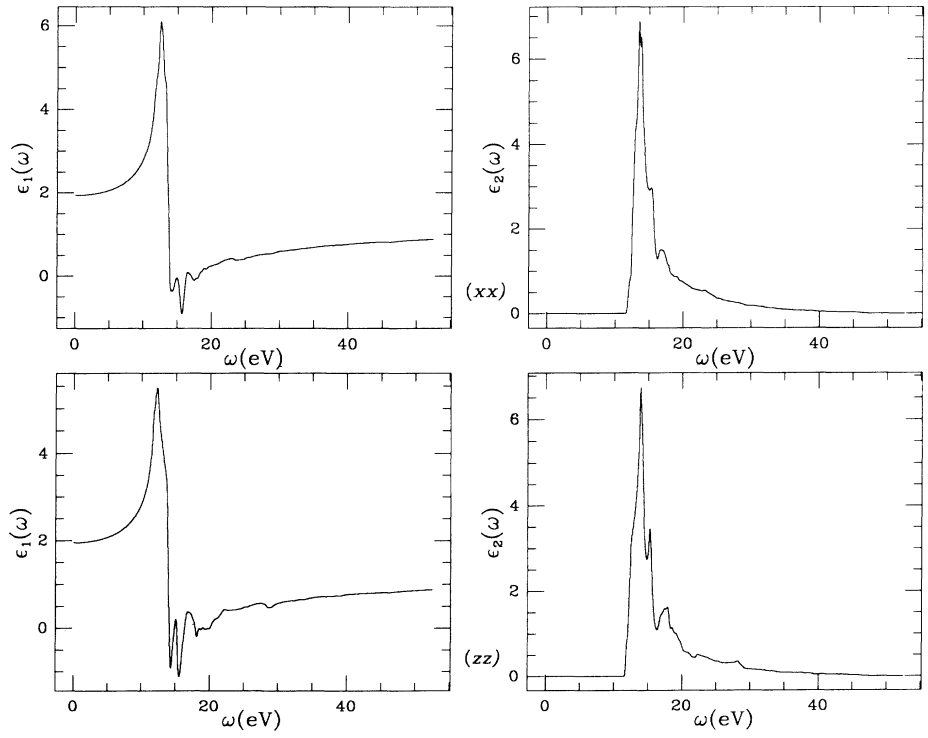

FIG. 3. Computed dielectric function for mhcp(S) at r_s=2.00 a.u. The top panels display the real (left) and imaginary (right) parts of $\epsilon_{xx}(\omega)$. The bottom panels present the same information for $\epsilon_{zz}(\omega)$.

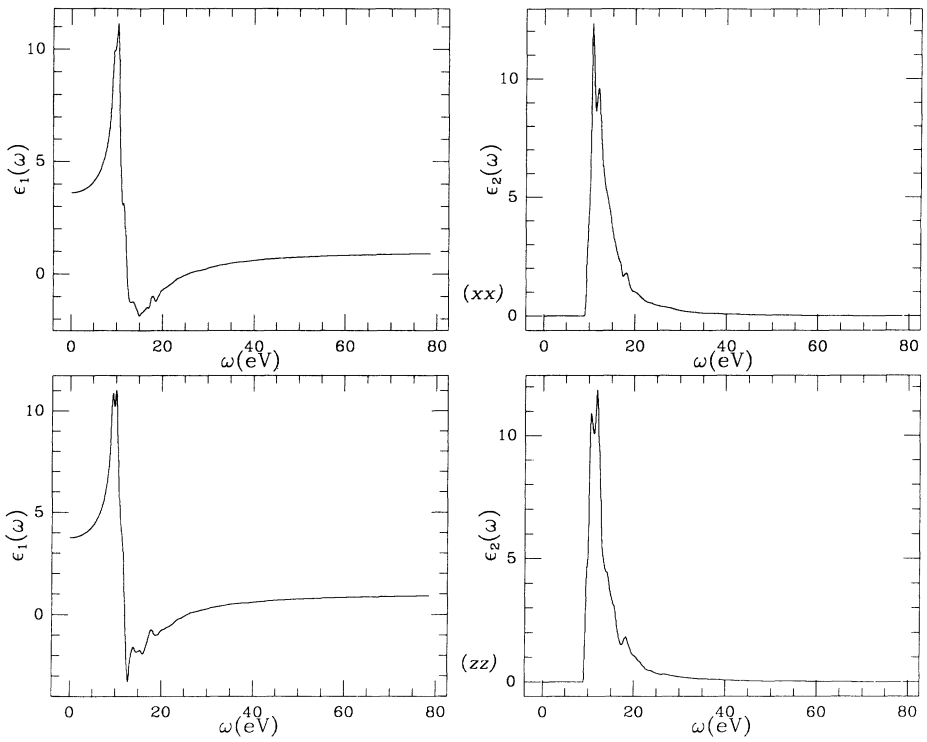

FIG. 4. Computed dielectric function for mhcp(S) at r_s=1.60 a.u. The top panels display the real (left) and imaginary (right) parts of $\epsilon_{xx}(\omega)$. The bottom panels present the same information for $\epsilon_{zz}(\omega)$.

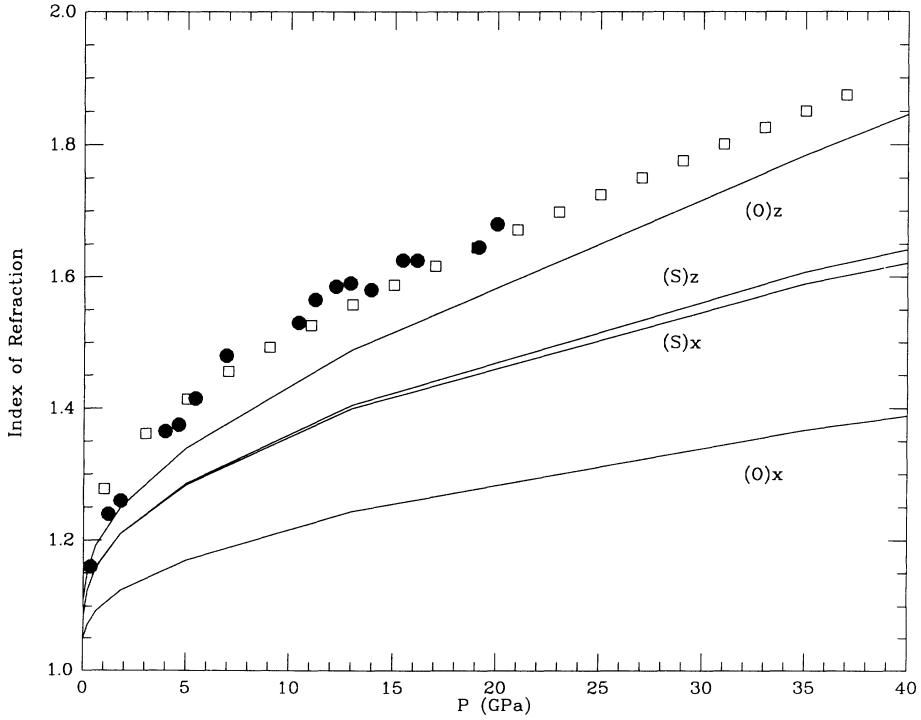

FIG. 5. Calculated index of refraction for 18 000 cm^{-1} photons as a function of pressure [lines marked (O)x and (O)z for mhcp(O), lines marked (S)x and (S)z for mhcp(S)] compared with experimental data from Ref. 19 (19 400 cm^{-1}, solid circles) and from Ref. 34 (18 000 cm^{-1}, open squares, representing a fit to the data).

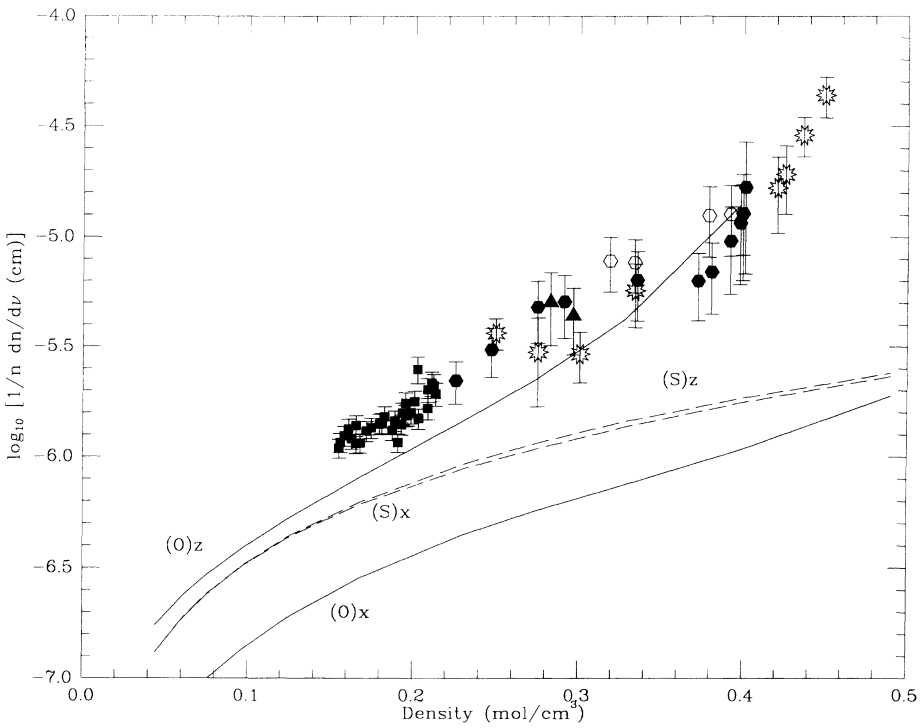

FIG. 6. Calculated $(1/n)dn/d\nu$ as a function of density [solid lines marked (O)x and (O)z for mhcp(O), dashed lines marked (S)x and (S)z for mhcp(S)] compared with experimental data from Ref. 22 (solid squares), Ref. 23 (solid triangles), Ref. 24 (open hexagons: room temperature, solid hexagons: 77 K) and this work (stars): 77 K.

sity, together with several experimental data sets. For mhcp(O) , the agreement is again quite good for the zz component, although the relevance of this fact is not clear in view of the uncertain sample conditions.[36] At the highest densities considered in our study (above approximately 200 GPa), the dispersion of n_{zz} for mhcp(O) turns out to be negative at the frequency chosen, which is consistent with the shift of the onset of direct interband absorption to lower frequencies.[37]

V. CONCLUSIONS

We have presented experimental data on the dielectric behavior of solid molecular hydrogen to pressures up to 220 GPa. To complement these measurements, we have carried out a calculation of the interband dielectric response of two structures for solid hydrogen. The chosen structures are only prototypes. In fact, recent total-energy calculations[38] have demonstrated that lower-energy structures exist. In this connection, it should be stated that current structural models treat the rotational degrees of freedom of the hydrogen molecules in a very simplified manner. For instance, the "dumbbell" wave function used for the "oriented" structures[39] is a linear combination of all the spherical harmonics. On the other hand, realistic models of ordered para-hydrogen at a high-pressure point to a mostly $J = 0$ wave function with a small admixture of $J = 2$, and ortho-hydrogen is mostly $J = 1$. Likewise, our simple spherical model may not be appropriate for a pure $J = 0$ crystal and, since the electrons can easily follow the molecular reorientations, is a rough description of a disordered system.

The study presented here provides a testing ground for calculations of the dielectric response. Through its application to a variety of structures, the method outlined should prove useful to interpret experimental data.

ACKNOWLEDGMENTS

Work at UCB-LBL was supported by the National Science Foundation (Grant No. DMR8818404), and by the Director, Office of Energy Research, Office of Basic Energy Sciences, Materials Sciences Division of the U.S. Department of Energy (Contract No. DE-AC03-76SF00098). Computer time was provided by the NSF at the Pittsburgh Supercomputer Center, and by the DOE at the Florida State University Computing Center. M.L.C. also acknowledges support from the J. S. Guggenheim Foundation. Work at Harvard was supported by the U.S. Air Force Phillips Laboratory (Contract No. F04611-89-K-0003). W.J.E. was also supported by the Fannie and John Hertz Foundation.

[1] E. Wigner and H. B. Huntington, J. Chem. Phys. **3**, 764 (1935).
[2] D. E. Ramaker, L. Kumar, and F. E. Harris, Phys. Rev. Lett. **34**, 812 (1975).
[3] C. Friedli and N. W. Ashcroft, Phys. Rev. B **16**, 662 (1977).
[4] B. I. Min, H. J. F. Jansen, and A. J. Freeman, Phys. Rev. B **33**, 6383 (1986).
[5] H. K. Mao, A. P. Jephcoat, R. J. Hemley, L. W. Finger, C. S. Zha, R. M. Hazen, and D. E. Cox, Science **239**, 1132 (1988).
[6] V. P. Glazkov, S. P. Besedin, I. N. Goncharenko, A. V. Irodova, I. N. Makarenko, V. A. Somenkov, S. M. Stishov, and S. Sh. Shil'steyn, Pis'ma. Zh. Eksp. Teor. Fiz. **47**, 661 (1988).
[7] R. J. Hemley, H. K. Mao, L. W. Finger, A. P. Jephcoat, R. M. Hazen, and C. S. Zha, Phys. Rev. B **42**, 6458 (1990).
[8] T. W. Barbee III, A. Garcia, M. L. Cohen, and J. L. Martins, Phys. Rev. Lett. **62**, 1150 (1989). This structure was first proposed for molecular hydrogen in A. A. Abrikosov, Astron. Zh. **31**, 112 (1954). It is also considered in S. Raynor, J. Chem. Phys. **87**, 2795 (1987).
[9] The LDA metallization pressure quoted in Ref. 5 is 40 GPa. Better estimates (see Ref. 8) put it at around 90 GPa. This should be compared with the 150–250-GPa values for the $Pa3$ structure (Refs. 2–4).
[10] R. J. Hemley and H. K. Mao, Phys. Rev. Lett. **61**, 857 (1988).
[11] H. E. Lorenzana, I. F. Silvera, and K. A. Goettel, Phys. Rev. Lett. **63**, 2080 (1989).
[12] H. K. Mao, R. J. Hemley, and M. Hanfland, Phys. Rev. Lett. **65**, 484 (1990).
[13] M. Hanfland, R. J. Hemley, and H. K. Mao, Phys. Rev. B **43**, 8767 (1991).
[14] J. H. Eggert, F. Moshary, W. J. Evans, H. E. Lorenzana, K. A. Goettel, I. F. Silvera, and W. C. Moss, Phys. Rev. Lett. **66**, 193 (1991).
[15] A. L. Ruoff and C. A. Vanderborgh, Phys. Rev. Lett. **66**, 754 (1991).
[16] See, for example, S. G. Louie and M. S. Hybertsen, Int. J. Quantum Chem.: Quantum Chem. Symp. **21**, 31 (1987), and references therein.
[17] A. Garcia, T. W. Barbee III, M. L. Cohen, and I. F. Silvera, Europhys. Lett. **13**, 355 (1990).
[18] H. Chacham and S.G. Louie, Phys. Rev. Lett. **66**, 64, (1991).
[19] H. Shimizu, E. M. Brody, H. K. Mao, and P. M. Bell, Phys. Rev. Lett. **47**, 128 (1981).
[20] J. van Straaten, R. J. Wijngaarden, and I. F. Silvera, Phys. Rev. Lett. **48**, 97 (1982).
[21] J. van Straaten and I. F. Silvera, Phys. Rev. B **37**, 6478 (1988).
[22] J. van Straaten and I. F. Silvera, Phys. Rev. B **37**, 1989 (1988).
[23] J. H. Eggert, K. A. Goettel, and I. F. Silvera, Europhys. Lett. **11**, 775 (1990); **12**, 381 (1990).
[24] R. J. Hemley, M. Hanfland, and H. K. Mao, Nature (London) **350**, 488 (1991).
[25] H. K. Mao, J. Xu, and P. M. Bell, J. Geophys. Res. **91**, 4673 (1986).
[26] J. C. Slater, Phys. Rev. **81**, 385 (1951).
[27] K. Inoue, H. Kanzaki, and S. Suga, Solid State Commun. **30**, 627 (1979).
[28] I. F. Silvera, Rev. Mod. Phys. **52**, 393 (1980).
[29] R. Natarajan and D. Vanderbilt, J. Comput. Phys. **81**, 218 (1989).
[30] F. Bassani and G. Pastori Parravicini, *Electronic States and Optical Transitions in Solids* (Pergamon, Oxford, 1975).
[31] G. Gilat and N. R. Bharatiya, Phys. Rev. B **12**, 3479 (1975).
[32] The Wigner-Seitz radius r_s satisfies the relation $(4\pi/3)r_s^3 = 1/n$, where n is the number density of electrons.
[33] We use the equation of state presented in Ref. 5 (extrapolated to higher densities when necessary).
[34] See Ref. 22, but note that there is a typographical error in the analytic fit for the index of refraction on p. 1994. The first coefficient should be 1.828, not 0.828.
[35] To fill in the 130 to 150 Gpa region we have used some data from Ref. 24, in which the contrast was better. An extrapolation of the index of refraction measured to 37 GPa (I. F. Silvera, NATO High Pressure Workshop, Pingree Park, CO, 1991) was used to convert to C values.
[36] For example, in our experiment we used unpolarized light on a sample of unknown status (single crystal, oriented powder, or random powder). If the sample were a single crystal oriented with the hexagonal axis perpendicular to the diamond culets, then the data should correspond to the xx $(= yy)$ component. With the hexagonal axis in the plane of the culets the measurements should reflect some average of xx and zz. Polycrystalline samples would likewise need suitable averages. We have chosen to display separately the xx and zz components to convey the most basic information.
[37] The same phenomenon is observed in n_{xx} at higher pressures, due to matrix element effects (see, for example, Figs. 1 and 2).
[38] E. Kaxiras, J. Broughton, and R. J. Hemley, Phys. Rev. Lett. **67**, 1138 (1991).
[39] Both our mhcp(O) and the structures treated in Ref. 38 fall in this category.